Large-scale production of aligned carbon nanotubes by the vapor phase growth method

Cheol Jin Lee [a],*, Seung Chul Lyu [a], Hyoun-Woo Kim [b], Chong-Yun Park [c], Cheol-Woong Yang [d]

[a] *Department of Nanotechnology, Hanyang University, 17 Haengdang-dong, Seongdong-gu, Seoul 133-791, Republic of Korea*
[b] *School of Materials Science and Engineering, Inha University, Incheon 402-751, Republic of Korea*
[c] *Department of Physics, Sungkyunkwan University, Suwon 440-746, Republic of Korea*
[d] *Department of Advanced Materials Engineering, Sungkyunkwan University, Suwon 440-746, Republic of Korea*

Abstract

Aligned multiwalled carbon nanotubes have been massively synthesized by the pyrolysis of iron pentacarbonyl $(Fe(CO)_5)$ and acetylene (C_2H_2) mixtures in a simply designed horizontal quartz tube reactor. The growth rate and the crystallinity of carbon nanotubes were enhanced by increasing the flow rate of Ar carrier gas. The growth rate, by adopting C_2H_2 direct bubbling, was dramatically increased compared with Ar direct bubbling, the maximum length of 2000 μm was achieved. © 2002 Elsevier Science B.V. All rights reserved.

1. Introduction

Carbon nanotubes (CNTs), since their first observation in 1991 [1], have been considered for many potential applications because of their extraordinary electrical and mechanical properties [2–4]. The CNTs can be used as a field emission electron source [5,6], a tip for scanning probe microscopy [7], and a hydrogen storage [8,9]. Synthesis of CNTs has been studied by various methods such as arc-discharge [10,11], laser vaporization [12], pyrolysis [13,14], plasma-enhanced chemical vapor deposition (CVD) [15,16], and thermal CVD [17–19].

From a viewpoint of applications, low cost, high-purity, high-yield, and large-scale production is important and thus, the vapor phase growth method has been studied intensively. Several research groups have employed the catalytic pyrolysis with iron/silica nanoparticles-C_2H_2 gas [20], a ferrocene–benzene mixture [21,22], a ferrocene–xylene mixture [23], a ferrocene–C_2H_2 mixture [24], and a $Fe(CO)_5$–C_2H_2 mixture [25].

In this work, we report a large-scale synthesis of high-purity CNTs using a catalytic reaction of $Fe(CO)_5$ and C_2H_2 mixtures at 750–950 °C. We supply a higher flow rate of Ar carrier gas, ranging from 2000 to 3000 standard cubic centimeters per minute (sccm) to obtain the high productivity of

* Corresponding author. Fax: +82-2-2296-1179.
E-mail address: cjlee@hanyang.ac.kr (C.J. Lee).

CNTs using a single-furnace system without a water-cooled injector. In addition, by C_2H_2 direct bubbling, we have realized a much higher yield of CNTs.

2. Experimental

A schematic diagram of a vapor phase growth system is shown in Fig. 1. It consists of a horizontal quartz tube furnace with an inner diameter of 20 mm and a heating zone of 200 mm.

The CNTs were synthesized by supplying the reaction gas (C_2H_2), the carrier gas (Ar), and the catalyst source ($Fe(CO)_5$) into the quartz tube. The liquid $Fe(CO)_5$, maintained at room temperature in the stainless steel bubbler, was injected by direct bubbling of Ar gas or C_2H_2 gas into the reactor. The flow rates of Ar and C_2H_2 gases for direct bubbling were 300 and 30 sccm, respectively. Gases and the catalyst source were directly introduced into the furnace at a temperature range of 750–950 °C for 30 min. A flow rate of Ar carrier gas ranged from 2000 to 3000 sccm. After the reaction, the furnace was cooled down to room temperature by flowing 500 sccm of Ar gas.

A scanning electron microscope (SEM) (Hitachi S-4700) was used to measure a length and a diameter of CNTs. A transmission electron microscopy (TEM) (JEOL, JEM-3011, 300 kV) was used to analyze a structure and a crystallinity of CNTs. The deposits were scraped off a wall of the quartz tube and then dispersed on a carbon TEM micro-

grid. A Raman spectrometer (Renishaw micro-Raman 2000) was also used to evaluate the crystallinity of CNTs. The 632.8 nm line of a He–Ne laser was used for excitation. A thermogravimetric analysis (TGA) (TGA 2050) was performed under flowing air with a heating rate of 5 °C/min.

3. Results and discussion

Large amounts of CNTs are synthesized using a $Fe(CO)_5$–C_2H_2 system and the products are deposited on the surface of the inside of the quartz tube. Fig. 2 shows the SEM micrographs for CNTs synthesized by Ar direct bubbling with a flow rate of 300 sccm. For the CNT growth, a flow rate of C_2H_2 gas is 30 sccm and a flow rate of Ar carrier gas ranges from 2000 to 3000 sccm for 30 min at 950 °C. Figs. 2a–c and d–f are micrographs of CNTs grown with an Ar flow rate of 2000 and 3000 sccm, respectively. The high-purity CNTs without carbonaceous particles are densely packed and uniformly grown on the inner surface of the quartz tube. The average lengths of CNTs are 500 and 720 μm, respectively, at Ar flow rate of 2000 and 3000 sccm. The length, which is proportional to the productivity of CNTs, is increased approximately 50% as the Ar flow rate increases from 2000 to 3000 sccm. The average diameters of CNTs are 70 and 100 nm at Ar flow rate of 2000 and 3000 sccm, respectively.

It is noteworthy that not only the deposits are found everywhere on the inner surface of the reactor, but the length and the diameter of those CNTs are homogeneous. High-purity CNTs without any trace of carbonaceous particles are produced. Moreover, the length of CNTs is much longer than that obtained by the previous work [25], due to a higher flow rate. In our experiments without a water-cooled injector, most iron catalyst condenses uniformly on the inside of the quartz tube where the temperature is sufficient for nanotube growth. It agrees with the previous results that the high Ar flow rate helps to produce the finer droplets of catalyst and thus, CNTs are distributed uniformly inside the reactor [22,26].

Decreasing the flow rate of Ar carrier gas below 2000 sccm results in shorter length of CNTs. From
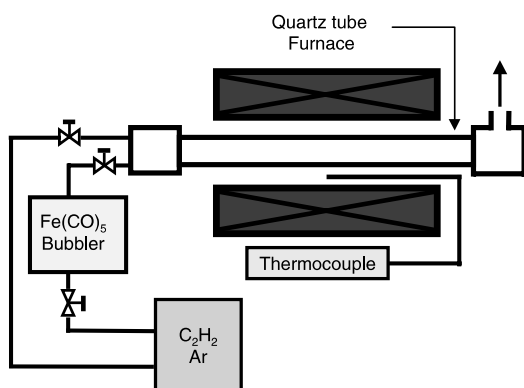

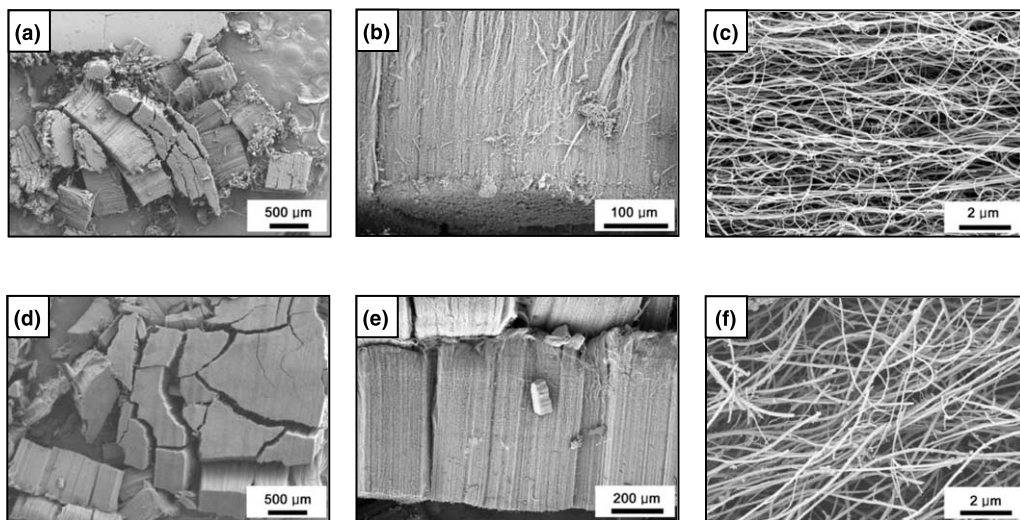Fig. 1. Schematic diagram of a vapor phase growth system.

Fig. 2. SEM micrographs for CNTs synthesized by Ar direct bubbling with the flow rate of 300 sccm. The flow rate of C_2H_2 gas is 30 sccm at 950 °C for 30 min. The high-purity CNTs without carbonaceous particles are produced. (a–c): The flow rate of Ar carrier gas is 2000 sccm. (d–f): The flow rate of Ar carrier gas is 3000 sccm. (a) SEM image of aligned CNTs with Ar flow rate of 2000 sccm, revealing the average length of about 500 μm. (b) Magnified view of (a). (c) Magnified view of (b), revealing the average diameter of about 70–75 nm. (d) SEM image of aligned CNTs with Ar flow rate of 3000 sccm, revealing the average length of about 720 μm. (e) Magnified view of (d). (f) Magnified view of (e), revealing the average diameter of about 100–110 nm.

the SEM analysis, the lengths are about 300 and 150 μm, respectively, at Ar flow rate of 1500 and 1000 sccm. We found homogeneously grown CNTs along the heating zone, regardless of growth temperature in the range of 750–950 °C. The growth rate decreases by decreasing the growth temperature.

Fig. 3 shows SEM micrographs for the CNTs synthesized at 950 °C by C_2H_2 direct bubbling. Both C_2H_2 gas and Ar carrier gas are flowed at 30 and 2000 sccm, respectively. The average length of CNTs is about 2000 μm, revealing that the length

drastically is increased by adopting C_2H_2 direct bubbling. There is no trace of carbonaceous particles on the CNTs using C_2H_2 direct bubbling. For the large-scaled CNT growth, we suggest that the adsorption probability between iron and carbon species increases in the case of C_2H_2 direct bubbling, thus the growth reaction is accelerated. Further study is necessary to understand a detailed mechanism.

Fig. 4 shows TEM images for CNTs synthesized by using Ar carrier gas of 2000 sccm at 950 °C. Fig. 4a shows that the CNTs, grown by Ar
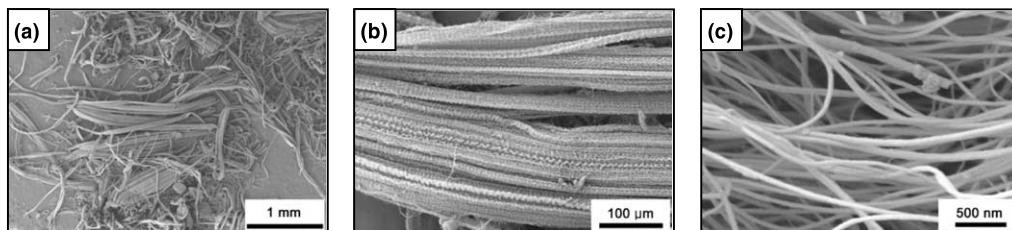

Fig. 3. SEM micrographs for CNTs synthesized by C_2H_2 direct bubbling with a flow rate of 30 sccm. The flow rate of Ar carrier gas is 2000 sccm at 950 °C for 30 min. High-purity CNTs without carbonaceous particles are produced. (a) SEM image of CNTs with the length of about 2000 μm. (b) Magnified view of (a). (c) Magnified view of (b), revealing the average diameter of about 80–90 nm.

direct bubbling, have a multiwalled structure with a hollow inside and no compartment layer in the tube. The outer diameter of the CNTs is almost constant over a long distance. Fig. 4b shows the CNTs grown by C_2H_2 direct bubbling, indicating a hollow inside and no compartment layer. Fig. 4c shows a high-resolution TEM (HRTEM) image of Fig. 4a, indicating a waving structure of graphite sheets at a short range. Fig. 4d is a HRTEM image of Fig. 4b, revealing a high degree of crystallinity. Most graphite sheets have straight fringes but the outer graphite sheets have waving fringes, indicating a defective crystalline structure. According to HRTEM images, the crystallinity of CNTs improves in the case of C_2H_2 direct bubbling compared with Ar direct bubbling.

TGA analysis is necessary to obtain the overall information on the crystalline perfection of CNTs. Fig. 5a is a plot for weight loss in percentage vs. oxidation temperature, measured by heating the CNTs in a TGA. The percentage weight loss curve between 200 and 800 °C is plotted by adjusting 100% for the weight loss at 800 °C, which is presumably the weight of the catalyst (usually 10% of total weight). The CNTs synthesized by Ar direct bubbling with Ar carrier gas of 2000 and 3000 sccm, start to gasify at approximately 400 °C (curve 1) and 470 °C (curve 2), respectively. The degree of crystalline perfection of CNTs becomes higher as the flow rate of Ar carrier gas increases. In the case of C_2H_2 direct bubbling, the CNTs start to gasify at approximately 500 °C (curve 3). According to TGA data, the crystallinity of graphite sheets by C_2H_2 direct bubbling is better than that of Ar direct bubbling.

Fig. 5b shows Raman spectra to evaluate the degree of crystallinity. All spectra show mainly two Raman bands at ~ 1335 cm^{-1} (D band) and ~ 1580 cm^{-1} (G band). The D band indicates the defective structure of graphite sheets [27]. The
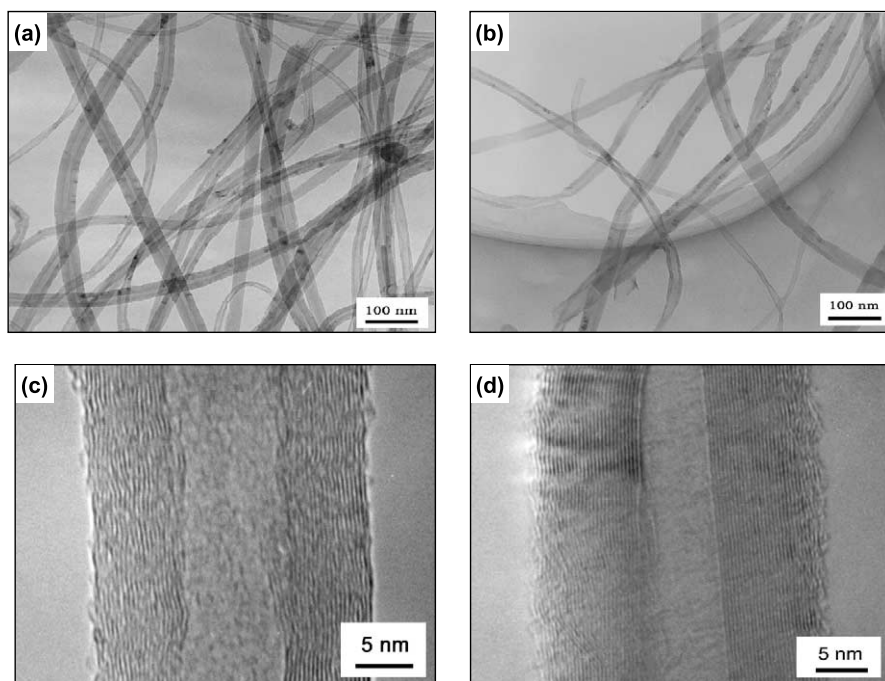

Fig. 4. TEM images for CNTs synthesized by Ar and C_2H_2 bubbling with Ar carrier gas of 2000 sccm. TEM image of CNTs shows a multiwalled structure with the hollow inside and no compartment layer in the tube. The outer diameter of the CNTs are almost constant over a long distance. (a) TEM image of CNTs synthesized by Ar direct bubbling. (b) TEM image of CNTs synthesized by C_2H_2 direct bubbling. (c) HRTEM image of (a), indicating a waving structure of graphite sheets at a short range. (d) HRTEM image of (b), indicating a good crystallinity of graphite sheets. The outer graphite sheets have a defective crystalline structure.
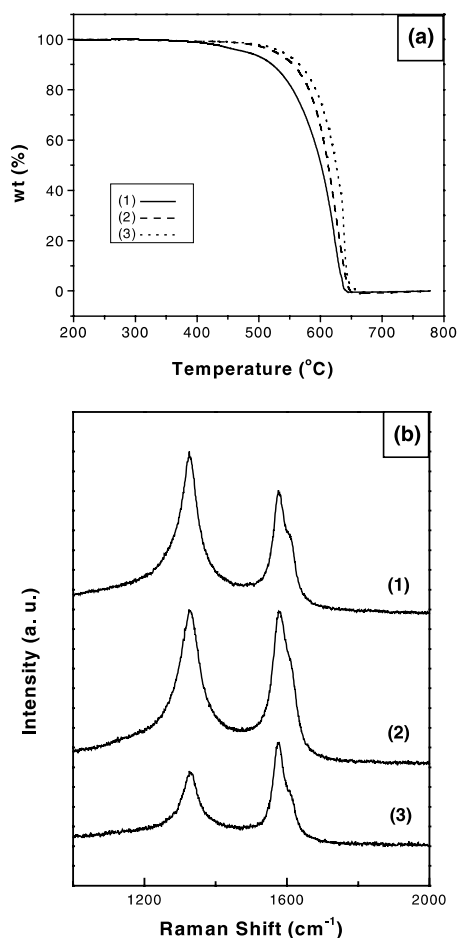
Fig. 5. (a) TGA data and (b) Raman spectra of the CNTs synthesized at 950 °C for 30 min. (1) Ar direct bubbling with Ar carrier gas of 2000 sccm. (2) Ar direct bubbling with Ar carrier gas of 3000 sccm. (3) C_2H_2 direct bubbling with Ar carrier gas of 2000 sccm. The CNTs synthesized by Ar direct bubbling with Ar carrier gas of 2000 and 3000 sccm start to gasify at 400 and 470 °C, respectively. The CNTs synthesized by C_2H_2 direct bubbling start to gasify at 500 °C. The crystallinity of CNTs improves by increasing the Ar flow rate and by adopting C_2H_2 direct bubbling.

peak intensity ratio of D and G bands decreases by increasing the flow rate of Ar carrier gas and by adopting C_2H_2 direct bubbling. These results mean that the crystallinity of CNTs improves by increasing the Ar flow rate and also advances by C_2H_2 direct bubbling instead of Ar direct bubbling. Raman spectra for the crystallinity of CNTs strongly agree with TGA data and HRTEM im-

ages. It is not clear why the crystallinity becomes better in the case of C_2H_2 direct bubbling. We surmise that Ar species used for bubbling may restrain the formation of carbon network at the initial stage, resulting in defective structures such as pentagons or heptagons. More systematic study is needed to explain the reason.

In summary, the well-aligned, high-purity CNTs are massively synthesized by vapor phase growth using the catalytic reaction of C_2H_2 and $Fe(CO)_5$ mixtures in the temperature range of 750–950 °C. Our method enables the deposition of CNTs along the total heating zone of the quartz tube without using the cold injector and realizes a mass production of high quality CNTs homogeneously using a higher flow rate of Ar carrier gas. In addition, C_2H_2 direct bubbling is a more effective method for the large-scale CNT growth, resulting in a length of 2000 μm. The crystallinity of graphite sheets is enhanced by increasing the flow rate of Ar carrier gas and by employing C_2H_2 direct bubbling.

Acknowledgements

References

[1] S. Iijima, Nature 354 (1991) 56.
[2] T.M. Whitney, J.S. Jiang, P.C. Searson, C.L. Chien, Science 261 (1993) 1316.
[3] M.M.J. Treacy, T.W. Ebbenson, J.M. Gibson, Nature 381 (1996) 678.
[4] P. Delaney, H.J. Choi, J. Ihm, S.G. Louie, M.L. Cohen, Nature 391 (1998) 466.
[5] W.A. de Heer, A. Chatelain, D. Ugarte, Science 270 (1995) 1179.
[6] Y. Saito, K. Hamaguchi, K. Hata, K. Uchida, Y. Tasaka, F. Ikazaki, M. Yumura, A. Kasuya, Y. Nishina, Nature 389 (1997) 554.
[7] H. Dai, J.H. Hafner, A.G. Rinzler, D.T. Colbert, R.E. Smalley, Nature 384 (1996) 147.
[8] C. Liu, Y.Y. Fan, M. Liu, H.T. Cong, H.M. Cheng, M.S. Dresselhaus, Science 286 (1999) 1127.
[9] P. Chen, X. Wu, J. Lin, K.L. Tan, Science 285 (1999) 91.

[10] D.S. Bethune, C.H. Kiang, M.S. deVries, G. Gorman, R. Savoy, J. Vazquez, R. Beyers, Nature 391 (1998) 466.

[11] C. Journet, W.K. Maser, P. Bernier, A. Loiseau, M. Lamy de la Chapelle, S. Lefrant, Nature 388 (1997) 756.

[12] A. Thess, R. Lee, P. Nikolaev, H. Dai, P. Petit, J. Robert, C. Xu, Y.H. Lee, S.G. Kim, D.T. Colbert, G. Scuseria, D. Tomanek, J.E. fisher, R.E. Smalley, Science 273 (1996) 483.

[13] M. Terrones, N. Grobert, J. Olivares, J.P. Zhang, H. Terrones, K. Kordatos, W.K. Hsu, J.P. Hare, P.D. Townsend, K. Prassides, A.K. Cheetham, H.W. Kroto, D.R.M. Walton, Nature 388 (1997) 52.

[14] R. Sen, A. Govindaraj, C.N.R. Rao, Chem. Phys. Lett. 267 (1997) 276.

[15] Z.F. Ren, Z.P. Huang, J.W. Xu, J.H. Wang, P. Bush, M.P. Siegal, P.N. Provencio, Science 282 (1998) 1105.

[16] L.C. Qin, D. Zhou, A.R. Krauss, D.M. Gruen, Appl. Phys. Lett. 72 (1998) 3437.

[17] S. Fan, M.G. Chapline, N.R. Franklin, T.W. Tombler, A.M. Cassell, H. Dai, Science 283 (1999) 512.

[18] C.J. Lee, D.W. Kim, T.J. Lee, Y.C. Choi, Y.S. Park, Y.H. Lee, W.B. Choi, N.S. Lee, G.S. Park, J.M. Kim, Chem. Phys. Lett. 312 (1999) 461.

[19] C.J. Lee, J.H. Park, J. Park, Chem. Phys. Lett. 323 (2000) 560.

[20] Z.W. Pan, S.S. Xie, B.H. Chang, C.Y. Wang, L. Lu, W. Liu, W.Y. Zhou, W.Z. Li, L.X. Qian, Nature 394 (1998) 632.

[21] H.M. Cheng, F. Li, X. Sun, S.D.M. Brown, M.A. Pimenta, A. Marucci, G. Dresselhaus, M.S. Dresselhaus, Chem. Phys. Lett. 289 (1998) 602.

[22] M. Mayne, N. Grobert, M. Terrones, R. Kamalakaran, M. Ruhle, H.W. Kroto, D.R.M. Walton, Chem. Phys. Lett. 338 (2001) 101.

[23] R. Andrews, D. Jacques, A.M. Rao, F. Derbyshire, D. Qian, X. Fan, E.C. Dickey, J. Chen, Chem. Phys. Lett. 303 (1999) 467.

[24] B.C. Satishkumar, A. Govindaraj, C.N.R. Rao, Chem. Phys. Lett. 307 (1999) 158.

[25] F. Rohmund, L.K.L. Falk, E.E.B. Campbell, Chem. Phys. Lett. 328 (2000) 369.

[26] R. Kamalakaran, M. Terrones, T. Seeger, Ph. Kohler-Redlich, M. Rühle, Y.A. Kim, T. Hayashi, M. Endo, Appl. Phys. Lett. 77 (2000) 3385.

[27] F. Tuinstra, J.L. Koenig, J. Chem. Phys. 53 (1970) 1126.